Theoretical and Mathematical Physics, **170**(2): 217–228 (2012)

PRECISE CHARM- AND BOTTOM-QUARK MASSES: THEORETICAL AND EXPERIMENTAL UNCERTAINTIES

© **K. G. Chetyrkin,[*] J. H. Kühn,[*] A. Maier,[*] P. Maierhöfer,[†] P. Marquard,[*] M. Steinhauser,[*] and C. Sturm[‡]**

We consider recent theoretical and experimental improvements in determining charm- and bottom-quark masses. We present a new, improved evaluation of the contribution of the gluon condensate $\langle\alpha_s G^2/\pi\rangle$ to the charm mass determination and a detailed study of potential uncertainties in the continuum cross section for $b\bar{b}$ production, together with a study of the parametric uncertainty from the α_s-dependence of our results. The final results, $m_c(3\,GeV) = 986(13)\,MeV$ and $m_b(m_b) = 4163(16)\,MeV$, together with the closely related lattice determination $m_c(3\,GeV) = 986(6)\,MeV$, currently represent the most precise determinations of these two fundamental standard-model parameters. We critically analyze the theoretical and experimental uncertainties.

Keywords: QCD sum rules, heavy quark mass, vacuum polarization

The past years have witnessed a significant improvement in determining charm- and bottom-quark masses as a consequence of improvements in experimental techniques and also in theoretical calculations. Quark mass determinations can be based both on a variety of experimental results and on theoretical calculations. One of the most precise methods currently is based on an idea advocated more than thirty years ago in [1]. We briefly review the most recent results obtained using this method. Interest in this approach was renewed after significant advances were achieved in higher-order perturbative calculations. In particular, the four-loop results (i.e., the coefficients $\overline{C}_n$ discussed below) are now available for the Taylor coefficients of the vacuum polarization, analytically up to $n = 3$ and numerically up to $n = 10$. The considered method uses the fact that the vacuum polarization function $\Pi(q^2)$ and its derivatives evaluated at $q^2 = 0$ can be regarded as short-range quantities with an inverse scale characterized by the distance between the reference point $q^2 = 0$ and the location of the threshold $q^2 = (3\,\mathrm{GeV})^2$ for the charm quark and $q^2 = (10\,\mathrm{GeV})^2$ for the bottom quark. This idea was used in [2] after the first three-loop evaluation of the moments became available [3]–[5]. The method was then further improved in [6] using the four-loop results [7], [8] for the lowest moment. An analysis that included the additional theoretical results in [9]–[11] and experimental results was presented in [12]. Here, we present an improved treatment of the contribution of the gluon condensate to the moments of the charm correlator and critically consider the behavior of the R ratio for the production of heavy quarks with the b flavor in the transition region from the threshold to the perturbative continuum and the related influence on finding the value of m_b.

We recall some basic notation and definitions. The vacuum polarization $\Pi_Q(q^2)$ induced by a heavy quark Q with the charge Q_Q (we do not take the so-called singlet contributions into account here) is an

[*]Institute for Theoretical Particle Physics, Karlsruhe Institute of Technology, Karlsruhe, Germany, e-mail: johann.kuehn@kit.edu.

[†]Institute for Theoretical Physics, University of Zurich, Zurich, Switzerland.

[‡]Max-Planck-Institut für Physik, Werner Heisenberg Institute, Munich, Germany.

Prepared from an English manuscript submitted by the authors; for the Russian version, see *Teoreticheskaya i Matematicheskaya Fizika*, Vol. 170, No. 2, pp. 265–279, February, 2012.

analytic function with poles and a branch cut at $q^2 = M^2_{J/\psi}$ for the charm quark (or $q^2 = M^2_\Upsilon$ for the bottom quark). Its Taylor coefficients $\overline{C}_n$ defined by

$$\Pi_Q(q^2) \equiv Q_Q^2 \frac{3}{16\pi^2} \sum_{n\geq 0} \overline{C}_n z^n$$

can currently be evaluated in perturbative QCD (pQCD) up to the order α_s^3. Here, $z \equiv q^2/4m_Q^2$, where $m_Q = m_Q(\mu)$ is the running $\overline{\rm MS}$ mass at the scale μ. Using a once-subtracted dispersion relation

$$\Pi_Q(q^2) = \frac{1}{12\pi^2} \int_0^\infty ds\, \frac{R_Q(s)}{s(s-q^2)},$$

where R_Q denotes the familiar R ratio for the production of heavy quarks with the flavor Q, we can express the Taylor coefficients in terms of the moments of R_Q. Equating perturbatively calculated and experimentally measured moments,

$$\mathcal{M}_n^{\rm exp} = \int \frac{ds}{s^{n+1}} R_Q(s), \tag{1}$$

leads to an (n-dependent) determination of the quark mass,

$$m_Q = \frac{1}{2}\left(\frac{9Q_Q^2}{4}\frac{\overline{C}_n}{\mathcal{M}_n^{\rm exp}}\right)^{1/2n}. \tag{2}$$

Significant progress has been made in evaluating the moments perturbatively since the first analysis in [1]. The $O(\alpha_s^2)$ contribution (three loops) was evaluated up to terms with $n = 8$ more than 13 years ago [3]–[5] and recently even up to $n = 30$ [13], [14]. The two lowest moments ($n = 0, 1$) of the vector correlator were evaluated in $O(\alpha_s^3)$, i.e., in the four-loop approximation [7], [8]. The two corresponding lowest moments for the pseudoscalar correlator were found using lattice simulations in [15] in order to obtain the charm-quark mass [16]. The second and third moments were evaluated for the vector, axial, and pseudoscalar correlators in [9], [10]. Finally, these results were combined with information about the threshold and high-energy behavior in the form of a Padé approximation, and the full q^2-dependence of all four correlators and the next moments from $n = 4$ up to $n = 10$ were reconstructed [11]. Moreover, the results were obtained with sufficient accuracy.

Most of the experimental input for both the charm and the bottom quarks was compiled and used in [6]. In [6], [12], an estimate for the gluon condensate was taken into account, giving a tiny contribution in the charm case. This estimate for the moments was obtained based on the results in [17] with the next-to-leading order (NLO) terms in [18] taken into account:

$$\delta\mathcal{M}_n^{\rm np} = \frac{12\pi^2 Q_c^2}{(4m_{c,\rm pole}^2)^{n+2}} \left\langle \frac{\alpha_s}{\pi} G^2 \right\rangle a_n \left(1 + \frac{\alpha_s}{\pi} b_n\right), \tag{3}$$

where

$$a_n = -\frac{2n+2}{15}\frac{\Gamma(n+4)}{\Gamma(4)}\frac{\Gamma(7/2)}{\Gamma(n+7/2)},$$

$$b_1 = \frac{135779}{12960}, \qquad b_2 = \frac{1969}{168}, \qquad b_3 = \frac{546421}{42525}, \qquad b_4 = \frac{661687433}{47628000}.$$

Using the $O(\alpha_s)$ pole-$\overline{\rm MS}$-mass conversion, i.e., the relation

$$\frac{m_Q(\mu)}{m_{Q,\rm pole}} = 1 - \frac{\alpha_s}{\pi}\left(\frac{4}{3} + \log\frac{\mu^2}{m_Q^2}\right),$$

we can express (3) in terms of the $\overline{\rm MS}$ mass at the scale $\mu = 3\,\text{GeV}$ with the new coefficients $\bar{b}_n = b_n - (2n+4)\big(4/3+\log(\mu^2/m_Q^2)\big)$. But because the mass appears in (3) with a high inverse power, this conversion becomes unstable[1] (although the effect obtained in [6], [12] was small, it nevertheless deserves attention). We therefore prefer to use the formulation in (3) directly on the mass shell with the parameters $m_{c,\text{pole}} = 1.5\,\text{GeV}$, $\alpha_s^{(4)}(3\,\text{GeV}) = 0.258$ (obtained from $\alpha_s^{(5)}(M_Z) = 0.1189$), and $\langle\alpha_s G^2/\pi\rangle = 0.006 \pm 0.012\,\text{GeV}^4$ [19].

The contributions to the moments are presented in Table 1 for both the leading-order (LO) and the NLO predictions; moreover, the contributions from the narrow resonances ($\mathcal{M}_n^{\text{res}}$), threshold ($\mathcal{M}_n^{\text{thresh}}$), and continuum ($\mathcal{M}_n^{\text{cont}}$) copied directly from [6] are presented in this table. The results for the charm-quark mass $m_c(3\,\text{GeV})$ are presented in Table 2, again for the two choices of the condensate contribution.

Table 1

n	$\mathcal{M}_n^{\text{res}}$ $\times 10^{(n-1)}$	$\mathcal{M}_n^{\text{thresh}}$ $\times 10^{(n-1)}$	$\mathcal{M}_n^{\text{cont}}$ $\times 10^{(n-1)}$	$\mathcal{M}_n^{\text{exp}}$ $\times 10^{(n-1)}$	$\mathcal{M}_n^{\text{np}}(\text{LO})$ $\times 10^{(n-1)}$	$\mathcal{M}_n^{\text{np}}(\text{NLO})$
1	0.1201(25)	0.0318(15)	0.0646(11)	0.2166(31)	−0.0001(3)	−0.0002(5)
2	0.1176(25)	0.0178(8)	0.0144(3)	0.1497(27)	−0.0002(5)	−0.0005(10)
3	0.1169(26)	0.0101(5)	0.0042(1)	0.1312(27)	−0.0004(8)	−0.0008(16)
4	0.1177(27)	0.0058(3)	0.0014(0)	0.1249(27)	−0.0006(12)	−0.0013(25)

Experimental moments in GeV^{-2n} as defined in (1), separated according to the contributions from the narrow resonances, the charm threshold region, and the continuum region above $\sqrt{s} = 4.8\,\text{GeV}$. The contribution from the gluon condensate in the LO and NLO are shown in the last two columns.

Table 2

n	$m_c(3\,\text{GeV})$ $[\text{np}_{\text{LO}}]$	$m_c(3\,\text{GeV})$ $[\text{np}_{\text{NLO}}]$	exp	α_s	μ	np_{LO}	np_{NLO}	total $[\text{np}_{\text{LO}}]$	total $[\text{np}_{\text{NLO}}]$
1	0.986	0.986	0.009	0.009	0.002	0.001	0.001	0.013	0.013
2	0.976	0.975	0.006	0.014	0.005	0.001	0.002	0.016	0.016
3	0.976	0.975	0.005	0.015	0.007	0.001	0.003	0.017	0.017
4	1.000	0.999	0.003	0.009	0.031	0.001	0.003	0.032	0.032

Results for $m_c(3\,\text{GeV})$ in GeV including the LO or NLO gluon condensate contribution. Errors are from experimental errors, the uncertainty of the constant α_s, the variation of μ, and the different options for the gluon condensate.

It can be seen from Tables 1 and 2 that the effect of the gluon condensate remains small, in particular, for the three lowest moments. The final result $m_c(3\,\text{GeV}) = 986(13)$ does not differ from the result in [6], [12]. The consistency of this result with the results for $n = 2, 3, 4$ can be regarded as additional confirmation of this value. Passing to the scale-invariant mass $m_c(m_c)$ [20] including the four-loop coefficients of the renormalization group functions, we have [12] $m_c(m_c) = 1279(13)\,\text{MeV}$. At this point, we recall that a recent study [21] in combination with a lattice simulation for the pseudoscalar correlator and also with the perturbative three- and four-loop results [5], [15], [10] has led to $m_c(3\,\text{GeV}) = 986(6)\,\text{MeV}$, which agrees remarkably with [6], [12]. Moreover, a fair agreement is also found with a recent analysis based on finite-energy sum rules using results up to the four-loop order in the perturbation theory [22], which leads to the result $m_c(3\,\text{GeV}) = 1008(26)\,\text{MeV}$.

[1] We thank S. Bodenstein for drawing our attention to this fact.

Until about two years ago, the only measurement of the cross section above but still close to the B-meson threshold, i.e., in the region between 10.6 and 11.2 GeV, had been performed by the CLEO collaboration in the mid-1980s [23]. Its large systematic uncertainty was responsible for a sizable fraction of the final error in m_b in the analysis in [6]. This measurement was superseded by results obtained by the BABAR collaboration [24] with a systematic error around 3%. In [12], the radiative corrections were unfolded and used to obtain a significantly improved determination of the moments. The CLEO and BABAR data are shown in Fig. 1 together with the theory prediction based on the pQCD in the order $O(\alpha_s^2)$. We note that $R_b(\sqrt{s})$ flattens out above 11.1 GeV, and we should therefore expect agreement between the pQCD and the experiment. The result for the region above 11.1 GeV is shown in Fig. 2, again with the theory prediction.

Averaging the data points above 11.1 GeV, we obtain $\overline{R}_b = 0.32$ with negligible statistical and uncorrelated systematic errors. The correlated systematic error is stated to be 3.5%. In [6], [12], data and pQCD were taken at face value for $\sqrt{s}$ respectively below and above 11.2 GeV (with linear interpolation between the last data point $R_b(11.2062\,\text{GeV}) = 0.331$ and the pQCD prediction $R_b^{\text{pQCD}}(11.24\,\text{GeV}) = 0.387$), yielding the moments and the quark masses presented in Tables 3 and 4.

Table 3

n	$\mathcal{M}_n^{\text{res,(1S-4S)}}$ $\times 10^{(2n+1)}$	$\mathcal{M}_n^{\text{thresh}}$ $\times 10^{(2n+1)}$	$\mathcal{M}_n^{\text{cont}}$ $\times 10^{(2n+1)}$	$\mathcal{M}_n^{\text{exp}}$ $\times 10^{(2n+1)}$
1	1.394(23)	0.287(12)	2.911(18)	4.592(31)
2	1.459(23)	0.240(10)	1.173(11)	2.872(28)
3	1.538(24)	0.200(8)	0.624(7)	2.362(26)
4	1.630(25)	0.168(7)	0.372(5)	2.170(26)

Moments for the bottom quark system in GeV^{-2n}.

Table 4

n	$m_b(10\,\text{GeV})$	exp	α_s	μ	total	$m_b(m_b)$
1	3.597	0.014	0.007	0.002	0.016	4.151
2	3.610	0.010	0.012	0.003	0.016	4.163
3	3.619	0.008	0.014	0.006	0.018	4.172
4	3.631	0.006	0.015	0.020	0.026	4.183

Results for $m_b(10\,\text{GeV})$ and $m_b(m_b)$ in GeV obtained from Eq. (2): the errors are from experimental errors, the uncertainty of α_s, and the variation of μ.

Our considerations are based on the assumption that the pQCD is valid in the region above ~ 11.2 GeV, where the relative momentum of b and $\bar{b}$ quarks has reached about 5 GeV. Indeed, from the behavior of R_b shown in Fig. 1, it is understandable that R_b, obviously, quickly reaches the level predicted by the pQCD. But in view of the 20% deviation between data and the pQCD around 11.2 GeV, we can consider the possibility that either the pQCD is valid only at significantly higher energies (case A) or the systematic error of the BABAR data is significantly underestimated, requiring a shift of the data by a sizeable amount (case B). These variants should be considered "worst case" scenarios. Nevertheless, we demonstrate that the resulting shifts are only slightly larger than the error quoted in [12]. We consider the two cases in detail.

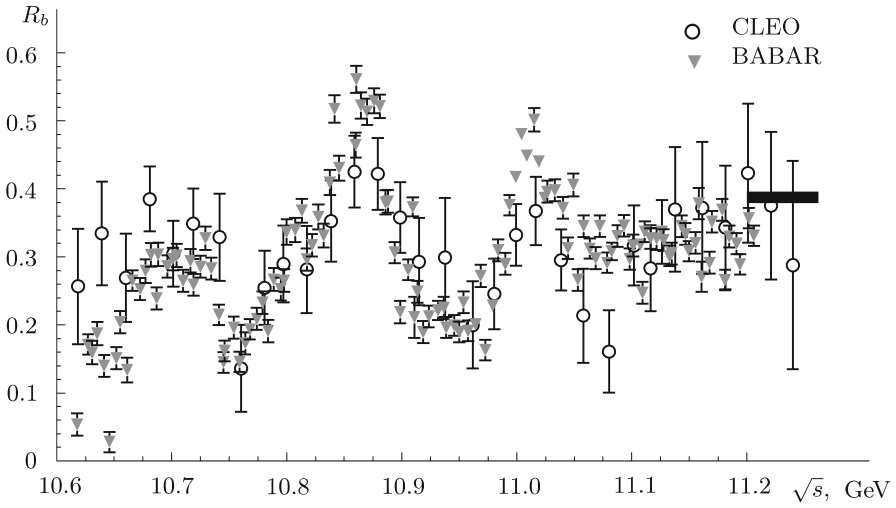

Fig. 1. Comparison of rescaled CLEO data (divided by 1.28) for R_b with BABAR data [12], [24]: the black bar on the right corresponds to the theory prediction [25].

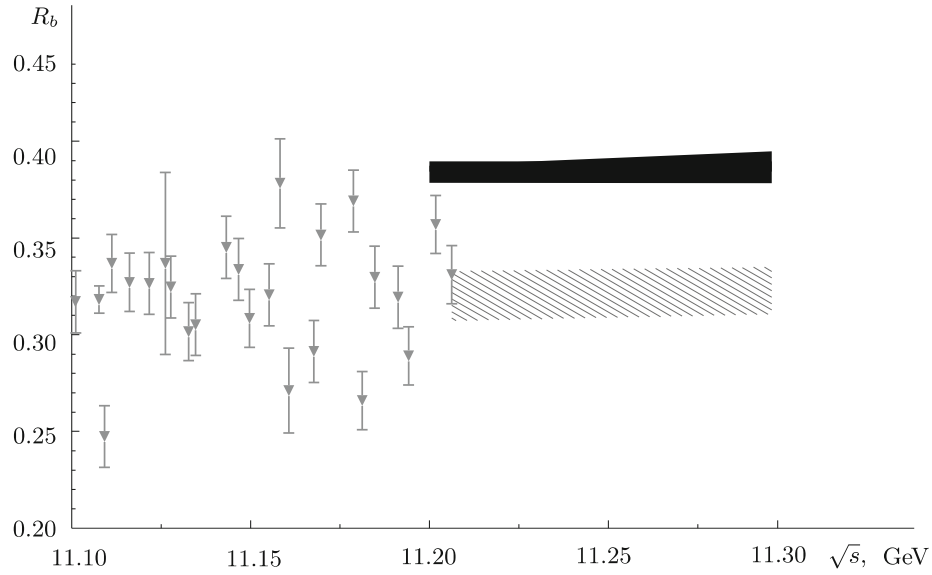

Fig. 2. The same data as in Fig. 1 in the region around $\sqrt{s} = 11.2\,\text{GeV}$ magnified: only the BABAR data is shown. The shaded band corresponds to a linear interpolation between $R(11.2062\,\text{GeV})$ and $R(13\,\text{GeV})$ (see case A in the text). The black bar on the right corresponds to the theory prediction [25].

Case A. We suppose that the pQCD holds only at higher energies, for example, above 13 GeV with linear interpolation between $R_b(11.2\,\text{GeV}) = 0.32$ and $R_b^{\text{pQCD}}(13\,\text{GeV}) = 0.377$. The results for the moments and $m_b(10\,\text{GeV})$ are shown in the respective Tables 5 and 6, assuming a 4% uncertainty at $\sqrt{s} = 11.2062\,\text{GeV}$ and no uncertainty for $R(13\,\text{GeV})$. A remarkable stability is observed for the bottom quark mass as can be seen from Table 6. For $n = 2$, we obtain $m_b(10\,\text{GeV}) = 3.630\,\text{GeV}$.

Case B: We suppose that the pQCD holds at 11.2 GeV and that the systematic error obtained in [24] is underestimated. Therefore, we rescale the data in the threshold region by the factor $R_b^{\text{pQCD}}/\overline{R}_b =$

Table 5

n	$\mathcal{M}_n^{\mathrm{res,(1S\text{-}4S)}}$ $\times 10^{(2n+1)}$	$\mathcal{M}_n^{\mathrm{thresh}}$ $\times 10^{(2n+1)}$	$\mathcal{M}_n^{\mathrm{cont}}$ $\times 10^{(2n+1)}$	$\mathcal{M}_n^{\mathrm{exp}}$ $\times 10^{(2n+1)}$
1	1.394(23)	0.270(11)	2.854(17)	4.518(31)
2	1.459(23)	0.226(9)	1.133(11)	2.819(27)
3	1.538(24)	0.190(8)	0.596(8)	2.324(26)
4	1.630(25)	0.159(6)	0.353(5)	2.142(26)

Moments for the bottom quark system in GeV^{-2n} obtained in case A: the contribution from the linear interpolation is contained in $\mathcal{M}_n^{\mathrm{cont}}$.

Table 6

n	$m_b(10\,\mathrm{GeV})$	exp	α_s	μ	total	$m_b(m_b)$
1	3.631	0.014	0.007	0.002	0.016	4.183
2	3.630	0.010	0.012	0.003	0.016	4.182
3	3.631	0.008	0.014	0.006	0.018	4.183
4	3.637	0.007	0.015	0.020	0.026	4.189

Bottom quark mass in GeV obtained in case A: the errors are from experimental errors, the uncertainty in α_s, and the variation of μ.

$0.387/0.32 \approx 1.21$ corresponding to a shift of about 7σ. We show the results for the moments in Table 7 and the corresponding predictions for $m_b(10\,\mathrm{GeV})$ in Table 8 with $m_b(10\,\mathrm{GeV}) = 3.592\,\mathrm{GeV}$ for $n = 2$. As expected, the trend of increasing m_b with increasing n already evident in Table 4 is even more pronounced.

As in the charm case, the result for the bottom-quark mass based on the lower moments is more stable than the result based on moments $n = 4$ and above. To suppress the theoretically evaluated input above 11.2 GeV (which corresponds to roughly 60% for the lowest, 40% for the second, and 26% for the third moment), we choose the result based on the second moment as our final result,

$$m_b(10\,\mathrm{GeV}) = 3610(16)\,\mathrm{MeV}, \tag{4}$$

which corresponds to $m_b(m_b) = 4163(16)$. We note that cases A and B are regarded as "worst case" scenarios; nevertheless, the respective shifts (for $n = 2$) are 20 MeV and -18 MeV, only slightly exceeding the 16 MeV uncertainty. We therefore use the original result (4). The explicit α_s-dependence of m_c and m_b can be found in [12]. In the ratio of charm- and bottom-quark masses, part of the dependence on α_s and on μ cancels:

$$\frac{m_c(3\,\mathrm{GeV})}{m_b(10\,\mathrm{GeV})} = 0.2732 - \frac{\alpha_\mathrm{s}(M_Z) - 0.1189}{0.002} \cdot 0.0014 \pm 0.0028.$$

This combination might be a useful input to the analysis of bottom decays.

In Fig. 3, we compare the results of this analysis with other results. The m_c value is obviously within the range obtained by other methods. Our result for m_b is slightly shifted toward the lower values, although it is still consistent with most other results.

Table 7

n	$\mathcal{M}_n^{\text{res,(1S-4S)}}$ $\times 10^{(2n+1)}$	$\mathcal{M}_n^{\text{thresh}}$ $\times 10^{(2n+1)}$	$\mathcal{M}_n^{\text{cont}}$ $\times 10^{(2n+1)}$	$\mathcal{M}_n^{\text{exp}}$ $\times 10^{(2n+1)}$
1	1.394(23)	0.347(14)	2.911(18)	4.651(32)
2	1.459(23)	0.290(12)	1.173(11)	2.921(28)
3	1.538(24)	0.242(10)	0.624(7)	2.404(27)
4	1.630(25)	0.203(8)	0.372(5)	2.205(27)

Moments for the bottom quark system in GeV^{-2n} obtained in case B.

Table 8

n	$m_b(10\,\text{GeV})$	exp	α_s	μ	total	$m_b(m_b)$
1	3.570	0.015	0.008	0.002	0.017	4.124
2	3.592	0.010	0.012	0.003	0.016	4.146
3	3.607	0.008	0.014	0.006	0.018	4.160
4	3.622	0.006	0.015	0.020	0.026	4.175

Bottom-quark mass in GeV obtained in case B: the errors are from experimental errors, the uncertainty in α_s, and the variation of μ.

The results presented in [12] constitute the most precise values for the charm- and bottom-quark masses available to date.[2] It is nevertheless tempting to indicate the dominant errors and thus identify potential improvements. In the case of the charm quark, the error is dominated by the parametric uncertainty in the strong coupling $\alpha_s(M_Z) = 0.1189 \pm 0.002$. The experimental and theoretical errors are comparable, the former being dominated by the electronic width of narrow resonances. In principle, this error could be further reduced by the high luminosity measurements at BESS III. A further reduction of the (already tiny) theoretical error, for example, by a five-loop calculation, seems difficult. Our results are additionally supported by comparison with the abovementioned results of numerical lattice calculations.

Improvements in determining the bottom-quark mass could come from experimental input, for example, through an improved determination of the electronic widths of the narrow Υ resonances or through a second, independent measurement of the R ratio in the region from $\Upsilon(4S)$ up to 11.2 GeV. We already discussed the slight mismatch between the theory prediction above 11.2 GeV and the data in the region below with their systematic error of about 3%. An independent measurement in the continuum region, for example, by the BELLE collaboration, would be extremely important. In this connection, it may be useful to collect the most important pieces of evidence supporting this remarkably small error. Part of the discussion is applicable to both charm and bottom quarks, and part is specific to only one of them. In particular, for charm (but also for bottom to some extent), the dependence of the result on μ increases for the higher moments beginning with $n = 4$ and dominates the total error. We therefore concentrate on the moments $n = 1, 2, 3$, which were used for the mass determination, and we mention the results for $n = 4$ only for illustration.

We begin with the charm quark. We immediately emphasize that the primary quantity to be determined

[2] A slightly more precise result for the charm quark was obtained in [21].

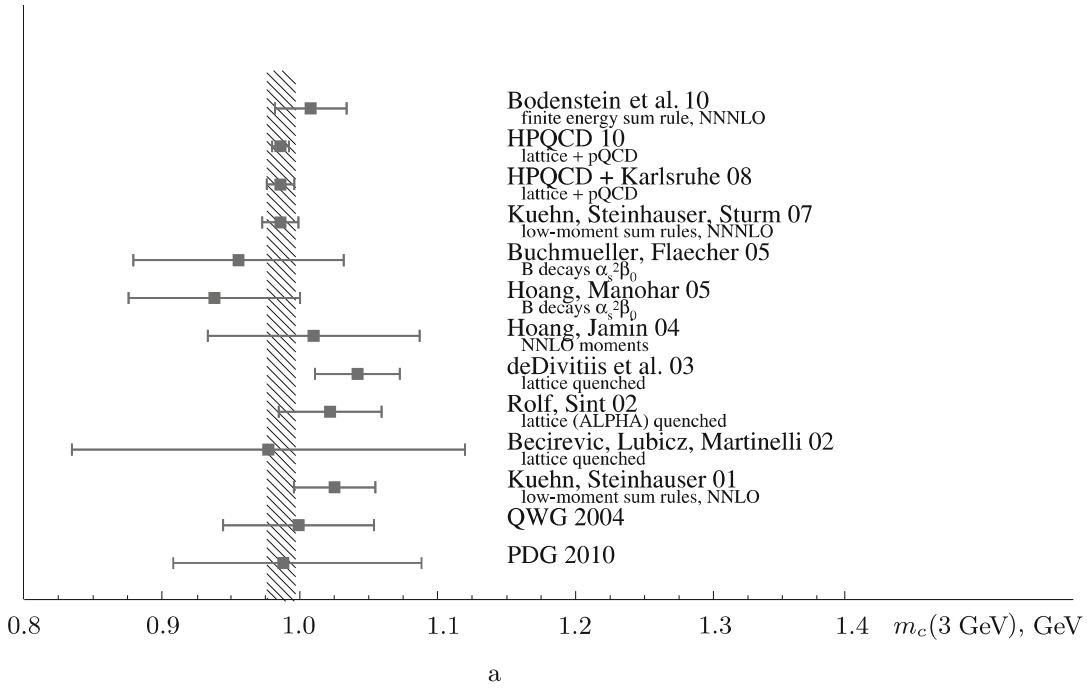

a

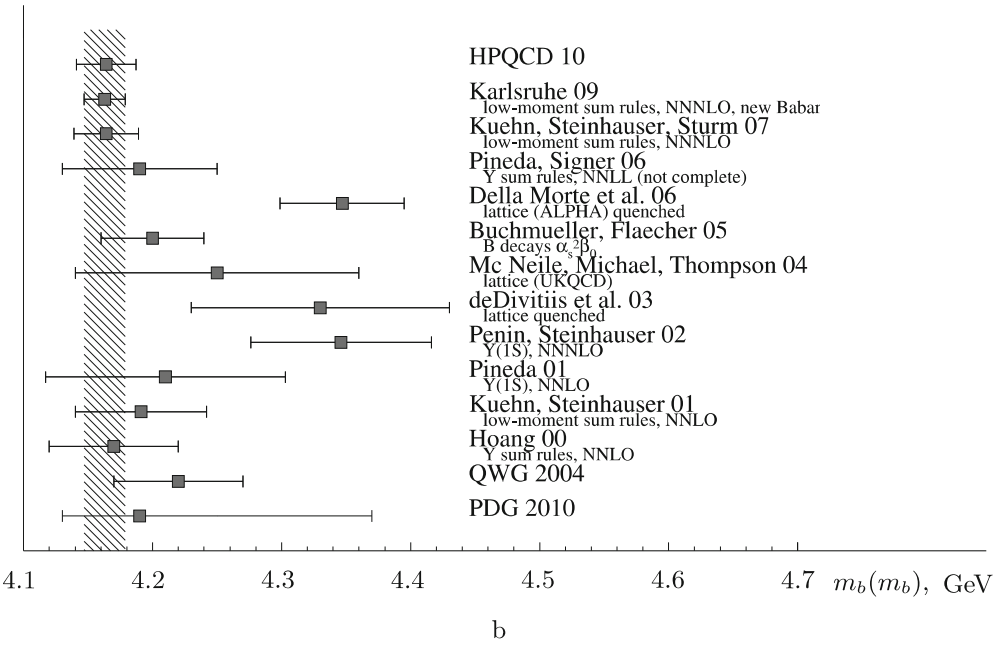

b

Fig. 3. Comparison of recent determinations of $m_c(3\,\mathrm{GeV})$ and $m_b(m_b)$: the shaded band indicates the values obtained in [12].

is the running mass at the 3 GeV scale, which is the scale characteristic for the production threshold and hence for the whole process. Furthermore, the strong coupling $\alpha_\mathrm{s}^{(4)}(3\,\mathrm{GeV}) = 0.258$ is already sufficiently small at this scale such that the higher-order terms in the perturbation series decrease rapidly. Last but not least, for many other processes of interest, such as B-meson decays into charm or processes involving virtual charm quarks such as $B \to X_\mathrm{s}\gamma$ or $K \to \pi\nu\bar{\nu}$, the characteristic scale is of the order of 3 GeV or

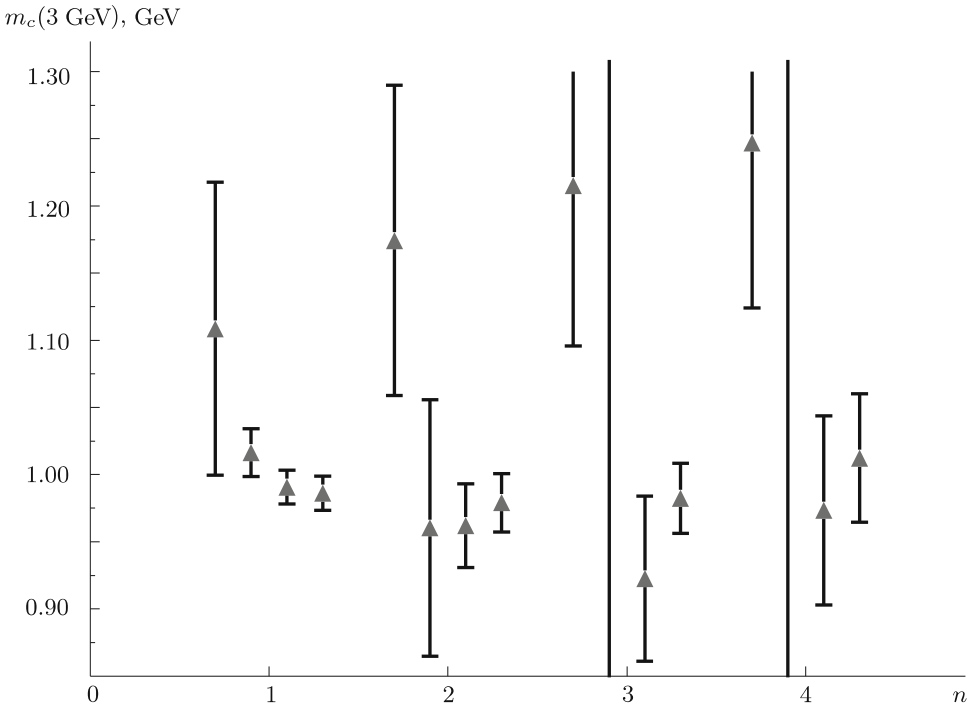

Fig. 4. Values of $m_c(3\,\mathrm{GeV})$ for $n = 1, 2, 3, 4$: for each value of n, the results from left to right correspond to including terms of the orders α_s^0, α_s^1, α_s^2, and α_s^3.

higher. Artificially running the mass first down to $O(1\,\mathrm{GeV})$ and then back to a higher scale thus leads to an unnecessary inflation of the error.

The theoretical uncertainty, resulting in particular from our ignorance of yet uncalculated higher orders, and the error in evaluating the experimental moments affects the quark mass determination. The former was estimated [6] by evaluating $m_c(\mu)$ at different renormalization scales between 2 and 4 GeV (of course, appropriately changing the coefficients $\overline{C}_n$) and subsequently evolving $m_c(\mu)$ to $m_c(3\,\mathrm{GeV})$. The error estimates based on these considerations are listed in Table 2.

The stability of the result under including higher orders is also evident in Fig. 4, where the results from different values of n are displayed separately in order of α_s^i with $i = 0, 1, 2, 3$. This argument can be made in more detail from the quantitative standpoint by rewriting (2) in the form[3]

$$m_c = \frac{1}{2}\left(\frac{9Q_c^2}{4}\frac{\overline{C}_n^{\mathrm{Born}}}{\mathcal{M}_n^{\mathrm{exp}}}\right)^{1/2n}(1 + r_n^{(1)}\alpha_\mathrm{s} + r_n^{(2)}\alpha_\mathrm{s}^2 + r_n^{(3)}\alpha_\mathrm{s}^3) \propto$$

$$\propto 1 - \begin{pmatrix}0.328\\0.524\\0.618\\0.662\end{pmatrix}\alpha_\mathrm{s} - \begin{pmatrix}0.306\\0.409\\0.510\\0.575\end{pmatrix}\alpha_\mathrm{s}^2 - \begin{pmatrix}0.262\\0.230\\0.299\\0.396\end{pmatrix}\alpha_\mathrm{s}^3, \qquad (5)$$

where the rows in the right-hand side correspond to the moments with $n = 1, 2, 3, 4$. We note that the coefficients decrease as the order of α_s increases. Estimating the relative error by $r_n^{\max}(\alpha_\mathrm{s}(3\,\mathrm{GeV}))^4$ leads to 1.4, 2.3, 2.7, 2.9‰ for $n = 1, 2, 3, 4$ and thus to an error estimate clearly smaller than the one based on the dependence on μ.

[3]The QED corrections are contained in $\overline{C}_n^{\mathrm{Born}}$.

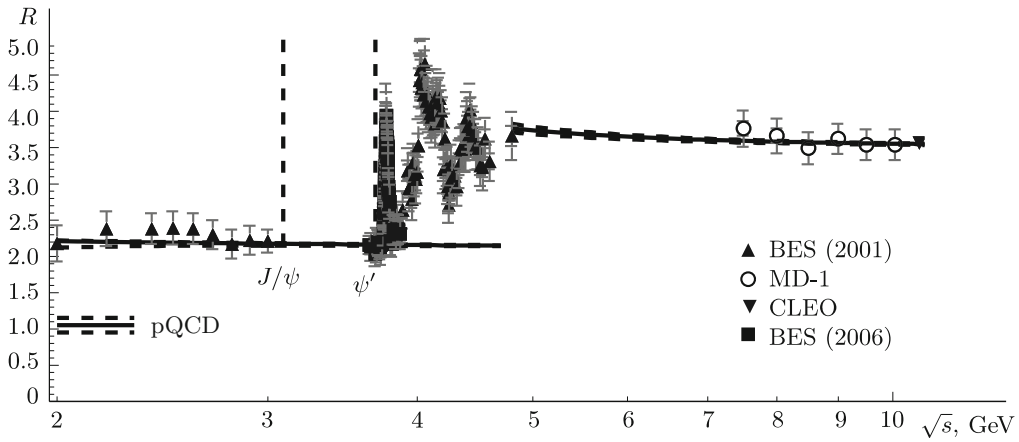

Fig. 5. The dependence $R(\sqrt{s})$ for different energy intervals around the charm threshold region: the solid line corresponds to the theoretical prediction.

The consistency between the results for different values of n is more evidence supporting our consideration (see Fig. 4 and Table 2). For the three lowest moments, the difference between the maximum and the minimum values amounts to only 10 MeV. This is a further indication of the self-consistency of our data set. We illustrate this aspect with a critical discussion of the "continuum contribution," i.e., the region above 4.8 GeV, where data points are available only at widely separated points. Instead of experimental data, we used the theoretical prediction for $R(s)$ to evaluate the contribution to the moments. If the true contribution from this region were shifted down by 10%, for example, then this would move the m_c value derived from $n = 1$ up by about 20 MeV. But this same shift would lead to a small increase by 3 MeV for $n = 2$ and leave the results for higher n practically unchanged. Furthermore, theoretical predictions and measurements in the region from 4.8 GeV up to the bottom-meson threshold, wherever available, are in excellent agreement, as shown in Fig. 5, with deviations well within the statistical and systematic errors of 3% to 5%. Last not least, the result described above agrees perfectly with the abovementioned recent results of numerical lattice calculations.

We now discuss the bottom quark with m_b evaluated at $\mu = 10\,\text{GeV}$. Again, we first study the stability of the perturbative expansion and then study the consistency of the experimental input. With $\alpha_s(10\,\text{GeV}) = 0.180$, the higher-order corrections decrease even more rapidly than in the charm case. Varying the scale μ between 5 GeV and 15 GeV leads to a completely negligible shift between 2 MeV and 6 MeV (see Table 4). As before, we can consider the analogue of Eq. (5) with the correction factor:

$$\frac{m_b}{m_b^{\text{Born}}} = 1 - \begin{pmatrix} 0.270 \\ 0.456 \\ 0.546 \\ 0.603 \end{pmatrix} \alpha_s - \begin{pmatrix} 0.206 \\ 0.272 \\ 0.348 \\ 0.410 \end{pmatrix} \alpha_s^2 + \begin{pmatrix} -0.064 \\ 0.048 \\ 0.051 \\ 0.012 \end{pmatrix} \alpha_s^3.$$

Taking $r_n^{\max}(\alpha_s(10\,\text{GeV}))^4$ for an error estimate leads to a relative error of 0.28, 0.48, 0.57, 0.63‰ for $n = 1, 2, 3, 4$, which is also smaller than our previous estimate.

We now turn to a critical discussion of the experimental data. The contribution from the four lowest Υ resonances was taken directly from the Particle Data Group data [26] with systematic errors obtained by linearly extrapolating the three lowest Υ resonances. The recent measurements of R_b in the threshold region up to 11.20 GeV [24] were analyzed in [12] and provided results consistent with the earlier analysis in [6] but led to a significant reduction of the error in the m_b value.

Compared with the charm analysis, analysis in the bottom case shows that a larger contribution arises from the region where experimental data are replaced with the theoretically predicted R_b with relative contributions of 63%, 41%, 26%, 17% for $n = 1, 2, 3, 4$. This is particularly characteristic of the lower moments. We therefore prefer to use the result for $n = 2$; as an alternative, we could also use the result for $n = 3$.

We collect the arguments for this approach:

1. For light and charmed quarks, the value of R predicted based on the pQCD works extremely well already in the region 2 to 3 GeV above threshold. No systematic deviation has been observed between theoretical and experimental results in the case of massless quarks starting from around 2 GeV and for the scattering cross section including the charm quark at energies equal to or above 5 GeV up to the threshold region for the bottom quark (see Fig. 5). It hence seems hard to expect that the same approach is doomed to fail when considering the production of bottom quarks.

2. If the true value of R_b in the continuum (above 11.2 GeV) significantly differed from value predicted by the theory, then the results for $n = 1, 2, 3$ would be mutually inconsistent. Specifically, a shift of the continuum term by 5% would move m_b derived from $n = 1, 2, 3$ respectively by about 64 MeV, 21 MeV, and 9 MeV.

We summarize. The charm- and bottom-quark mass determinations have made significant progress in recent years. A further reduction of the theoretical and experimental error seems difficult at present, but independent experimental results on the R ratio would help to further consolidate the current situation. The confirmation obtained using a recent lattice calculation with similarly small uncertainty gives additional confidence in the result for m_c.

Acknowledgments. One of the authors (J. H. K.) thanks the organizers of the XVI International Seminar on High Energy Physics "Quarks-2010" for the hospitality.

This work was supported by the Deutsche Forschungsgemeinschaft (Project No. SFB/TR-9 "Computational Particle Physics") and in part (C. S.) by the European Community's Marie Curie Research Training Network *Tools and Precision Calculations for Physics Discoveries at Colliders* (HEPTOOLS Contract No. MRNT-CT-2006-035505).

REFERENCES

1. M. A. Shifman, A. I. Vainshtein, and V. I. Zakharov, *Nucl. Phys. B*, **147**, 385–447 (1979).
2. J. H. Kühn and M. Steinhauser, *Nucl. Phys. B*, **619**, 588–602 (2001); Erratum, **640**, 415 (2002); arXiv:hep-ph/0109084v3 (2001).
3. K. G. Chetyrkin, J. H. Kühn, and M. Steinhauser, *Phys. Lett. B*, **371**, 93–98 (1996); arXiv:hep-ph/9511430v1 (1995).
4. K. G. Chetyrkin, J. H. Kühn, and M. Steinhauser, *Nucl. Phys. B*, **482**, 213–240 (1996); arXiv:hep-ph/9606230v1 (1996).
5. K. G. Chetyrkin, J. H. Kühn, and M. Steinhauser, *Nucl. Phys. B*, **505**, 40–64 (1997); arXiv:hep-ph/9705254v1 (1997).
6. J. H. Kühn, M. Steinhauser, and C. Sturm, *Nucl. Phys. B*, **778**, 192–215 (2007); arXiv:hep-ph/0702103v1 (2007).
7. K. G. Chetyrkin, J. H. Kühn, and C. Sturm, *Eur. Phys. J. C*, **48**, 107–110 (2006); arXiv:hep-ph/0604234v2 (2006).
8. R. Boughezal, M. Czakon, and T. Schutzmeier, *Phys. Rev. D*, **74**, 074006 (2006); arXiv:hep-ph/0605023v3 (2006).

9. A. Maier, P. Maierhofer, and P. Marqaurd, *Phys. Lett. B*, **669**, 88–91 (2008); arXiv:0806.3405v2 [hep-ph] (2008).
10. A. Maier, P. Maierhofer, P. Marquard, and A. V. Smirnov, *Nucl. Phys. B*, **824**, 1–18 (2010); arXiv:0907.2117v1 [hep-ph] (2009).
11. Y. Kiyo, A. Maier, P. Maierhöfer, and P. Marquard, *Nucl. Phys. B*, **823**, 269–287 (2009); arXiv:0907.2120v1 [hep-ph] (2009).
12. K. G. Chetyrkin, J. H. Kühn, A. Maier, P. Maierhöfer, P. Marquard, M. Steinhauser, and C. Sturm, *Phys. Rev. D*, **80**, 074010 (2009); arXiv:0907.2110v1 [hep-ph] (2009).
13. R. Boughezal, M. Czakon, and T. Schutzmeier, *Nucl. Phys.* (Proc. Suppl.), **160**, 160–164 (2006); arXiv:hep-ph/0607141v1 (2006).
14. A. Maier, P. Maierhöfer, and P. Marquard, *Nucl. Phys. B*, **797**, 218–242 (2008).
15. C. Sturm, *JHEP*, **0809**, 075 (2008); arXiv:0805.3358v1 [hep-ph] (2008).
16. I. Allison et al. (HPQCD Collab.), *Phys. Rev. D*, **78**, 054513 (2008); arXiv:0805.2999v2 [hep-lat] (2008).
17. V. A. Novikov, L. B. Okun, M. A. Shifman, A. I. Vainshtein, M. B. Voloshin, and V. I. Zakharov, *Phys. Rep.*, **41**, 1–133 (1978).
18. D. J. Broadhurst, P. A. Baikov, V. A. Ilyin, J. Fleischer, O. V. Tarasov, and V. A. Smirnov, *Phys. Lett. B*, **329**, 103–110 (1994); arXiv:hep-ph/9403274v1 (1994).
19. B. L. Ioffe, *Prog. Part. Nucl. Phys.*, **56**, 232–277 (2006); arXiv:hep-ph/0502148v2 (2005).
20. K. G. Chetyrkin, J. H. Kühn, and M. Steinhauser, *Comput. Phys. Commun.*, **133**, 43–65 (2000); arXiv:hep-ph/0004189v1 (2000).
21. C. McNeile, C. T. H. Davies, E. Follana, K. Hornbostel, and G. P. Lepage, *Phys. Rev. D*, **82**, 034512 (2010); arXiv:1004.4285v1 [hep-lat] (2010).
22. S. Bodenstein, J. Bordes, C. A. Dominguez, J. Peñarrocha, and K. Schilcher, *Phys. Rev. D*, **82**, 114013 (2010); arXiv:1009.4325v2 [hep-ph] (2010).
23. D. Besson et al. (CLEO Collab.), *Phys. Rev. Lett.*, **54**, 381–384 (1985).
24. B. Aubert et al. (BABAR Collab.), *Phys. Rev. Lett.*, **102**, 012001 (2009); arXiv:0809.4120v1 [hep-ex] (2008).
25. R. V. Harlander and M. Steinhauser, *Comput. Phys. Commun.*, **153**, 244–274 (2003); arXiv:hep-ph/0212294v3 (2002).
26. W.-M. Yao et al. (Particle Data Group), *J. Phys. G*, **33**, 1–1232 (2006); arXiv:astro-ph/0601168v2 (2006).